Development 137, 1731-1741 (2010) doi:10.1242/dev.049197

Dysregulation of cell-to-cell connectivity and stomatal patterning by loss-of-function mutation in *Arabidopsis CHORUS* (*GLUCAN SYNTHASE-LIKE 8*)

Jessica M. Guseman[1], Jin Suk Lee[1], Naomi L. Bogenschutz[1,*], Kylee M. Peterson[1], Rebecca E. Virata[1], Bo Xie[2], Masahiro M. Kanaoka[3], Zonglie Hong[2] and Keiko U. Torii[1,4,†]

Summary

Patterning of stomata, valves on the plant epidermis, requires the orchestrated actions of signaling components and cell-fate determinants. To understand the regulation of stomatal patterning, we performed a genetic screen using a background that partially lacks stomatal signaling receptors. Here, we report the isolation and characterization of *chorus* (*chor*), which confers excessive proliferation of stomatal-lineage cells mediated by *SPEECHLESS* (*SPCH*). *chor* breaks redundancy among three *ERECTA* family genes and strongly enhances stomatal patterning defects caused by loss-of-function in *TOO MANY MOUTHS*. *chor* seedlings also exhibit incomplete cytokinesis and growth defects, including disruptions in root tissue patterning and root hair cell morphogenesis. *CHOR* encodes a putative callose synthase, GLUCAN SYNTHASE-LIKE 8 (GSL8), that is required for callose deposition at the cell plate, cell wall and plasmodesmata. Consistently, symplastic macromolecular diffusion between epidermal cells is significantly increased in *chor*, and proteins that do not normally move cell-to-cell, including a fluorescent protein-tagged SPCH, diffuse to neighboring cells. Such a phenotype is not a general trait caused by cytokinesis defects. Our findings suggest that the restriction of symplastic movement might be an essential step for the proper segregation of cell-fate determinants during stomatal development.

KEY WORDS: *Arabidopsis*, Stomatal patterning, Callose synthase, Plasmodesmata, Cytokinesis

INTRODUCTION

The generation of tissue patterns in multicellular organisms requires coordinated cell proliferation and differentiation. Encapsulated by cell walls, pattern formation in plants occurs in the absence of cell migration. The last step of plant cell division, cytokinesis, is marked by a cell plate separating the two daughter cells. It is thought that positional information instructs the newly divided plant cells to acquire specific cell fate. One mechanism for transmitting and receiving such information is receptor kinase-mediated signaling, in which secreted ligands diffusing through the apoplast are received by receptors in neighboring cells. Plants possess large numbers of receptor-like kinases (RLKs) to regulate diverse aspects of development (Dievart and Clark, 2004; Shiu and Bleecker, 2001; Torii and Clark, 2000). The second mechanism is direct cell-to-cell movement of regulatory molecules, such as transcription factors and RNAs, through the symplastic continuum via plasmodesmata (Lucas and Lee, 2004; Oparka and Roberts, 2001).

Stomatal patterning has emerged as a model in which to study how positional cues influence functional tissue patterning. In *Arabidopsis*, stomata differentiate from a subset of protodermal cells called meristemoid mother cells (MMCs). An MMC undergoes an asymmetric entry division that creates a meristemoid and a larger sister cell called a stomatal lineage ground cell (SLGC). The meristemoid reiterates a few rounds of asymmetric cell divisions that amplify surrounding SLGCs. The meristemoid eventually differentiates into a guard mother cell (GMC) that divides symmetrically to form two guard cells constituting a stoma (Bergmann and Sack, 2007; Nadeau and Sack, 2002b). The SLGCs might differentiate into pavement cells or become MMCs, which initiate additional stomatal cell lineages.

Molecular genetic studies have revealed both positive and negative regulators of stomatal development. Three closely-related basic helix-loop-helix (bHLH) proteins, SPEECHLESS (SPCH), MUTE and FAMA, specify the initiation of the stomatal lineage, differentiation of meristemoids to GMCs, and the terminal differentiation of guard cells, respectively, together with SCREAM (SCRM; also known as ICE1) and SCRM2 bHLH proteins (Kanaoka et al., 2008; MacAlister et al., 2007; Ohashi-Ito and Bergmann, 2006; Pillitteri et al., 2008; Pillitteri et al., 2007). Two Myb proteins restrict the division of GMCs (Lai et al., 2005). A ligand-receptor signaling pathway inhibits entry into the stomatal lineage and orients asymmetric division. The components of the pathway include putative ligands, EPIDERMAL PATTERNING FACTOR 1 (EPF1) and EPF2, a putative receptor, TOO MANY MOUTHS (TMM), three redundant receptor-like kinases, ERECTA (ER), ERECTA-LIKE 1 (ERL1) and ERL2, and mitogen-activated protein kinase cascades mediated via YODA, MKK4/5 and MPK3/6 (Bergmann et al., 2004; Hara et al., 2007; Hara et al., 2009; Hunt and Gray, 2009; Nadeau and Sack, 2002a; Shpak et al., 2005; Wang et al., 2007). It remains unclear how the actions of these positive and negative regulators are spatially coordinated during epidermal development.

[1]Department of Biology, University of Washington, Seattle, WA 98195, USA. [2]Department of Microbiology, Molecular Biology and Biochemistry, University of Idaho, Moscow, ID 83844, USA. [3]Division of Biological Science, Graduate School of Science, Nagoya University, Nagoya, Aichi 464-8602, Japan. [4]PREST, Japan Science and Technology Agency, Tokyo, Japan.

*Present address: Molecular and Cellular Biology Graduate Program, University of Washington, Seattle, WA 98195, USA
†Author for correspondence (ktorii@u.washington.edu)

Accepted 1 March 2010

To better understand the regulation of stomatal patterning, we performed a sensitized genetic screen using *er erl1* as a starting background. We report a new stomatal patterning mutant, *chorus* (*chor*). *CHOR* represents a weak allele of the putative callose synthase gene *GSL8* (also known as *CALLOSE SYNTHASE 10*), which was recently shown to be required for cytokinesis (Chen et al., 2009; Thiele et al., 2009). Although Chen et al. also observed that *gsl8* mutants show stomatal patterning defects, both the exact nature of the defects and the mechanism by which loss-of-function mutations in a callose synthase gene leads to stomatal clustering remain unclear. On the basis of histochemical callose deposition and cell-to-cell diffusion assays, we suggest a potential role of plasmodesmatal macromolecular trafficking as a mechanism for proper stomatal patterning.

MATERIALS AND METHODS

Plant materials

Arabidopsis thaliana Columbia (Col) accession was used as a wild type. Mutants and lines used in this study were in the Col background unless otherwise specified. The *chor* mutant was derived from an EMS (ethyl methanesulfonic acid)-mutagenized *er-105 erl1-2* population and was outcrossed three times to wild type before analysis. The *er-105 erl1-2* background possesses an additional *gl1* mutation, which confers trichomeless leaves. A T-DNA insertion allele of *GSL8* (*gsl8-2*; GK 851 C04) was obtained from the Nottingham Arabidopsis Stock Centre (NASC). The following transgenic lines and mutants have been described previously: *proERL1::GUS*, *proTMM::GUS*, *er-105*, *erl1-2*, *er-105 erl1-2* and *er-105 erl1-2 erl2-1* (Shpak et al., 2004; Shpak et al., 2005); *spch-3* (Pillitteri et al., 2007); *tmm-1* and *proTMM:GUS-GFP* (Nadeau and Sack, 2002a); *proMUTE::GFP* (Pillitteri et al., 2008); *proCaMV35S:YFP-PDCB1* (Simpson et al., 2009); *atnack1-1* (Nishihama et al., 2002); and *scd1-2* (Falbel et al., 2003). The transgenes and known mutant alleles were introduced into *chor*/+ via genetic crosses. Seedlings were grown in modified Murashige-Skoog media with 1×Gamborg B5 vitamins and 1% w/v sucrose at 21°C under long-day conditions (18/6 light-dark cycle). Plates (90 mm diameter, 25 mm thickness) were sealed with surgical tape (Micropore, 3M) to minimize condensation.

Genetic screen

er-105 erl1-2 seeds were treated with 0.3% (v/v) EMS overnight. Seeds were harvested from individual M1 plants, and 528 M2 seed populations were visually screened for seedling epidermal phenotypes.

Genotyping

Mutant genotypes were verified by PCR-based analyses. The *chor* mutant allele was detected by derived Cleavage Amplified Polymorphic Sequence (dCAPS) (Neff et al., 1998), using the primer pair chorus dCAPS F-NlaIV and chorus dCAPS R-NlaIV, and subsequent digestion with *Nla*IV. The T-DNA insertion site of *gsl8-2* was detected by the primer pair At2g36850 M18F and GABI-K o8409. See Table S1 in the supplementary material for primer sequences. Genotyping of *er-105*, *erl1-2*, *erl2-1*, *tmm-1* and *spch-3* has been described previously (Lukowitz et al., 2004; Pillitteri et al., 2007; Shpak et al., 2004).

Map-based cloning of *CHORUS*

A mapping population of *chor* was generated by crossing B1F1 *chor*/+ *er erl1* to L*er*. Initially, a bulked segregant analysis (Lukowitz et al., 2000) was performed using a combined pool of 33 *chor* seedlings from the mapping population, which revealed the strong linkage of *chor* to the mid-bottom of chromosome 2 at SSLP markers MSAT2.36 and MSAT2.9 (Loudet et al., 2002). Further fine mapping was performed within this interval using two SSLP markers (KTL T20F21 and KTL F3G5) and a total of 1831 F2 *chor* (–/–) seedlings, which located *CHOR* within the ~145-kb interval encompassing the BACs F13K3 and T1J8. All 36 predicted open-reading frames within this interval were sequenced, and this led to the identification of a single G→A substitution at position 13447 of At2g36850, which encodes *GSL8* (*CalS10*). The SSLP, CAPS, and dCAPS markers for map-based cloning of *CHOR* were designed based on the information available in Monsanto *Arabidopsis* Polymorphism and L*er* Sequence Collection (http://www.Arabidopsis.org/Cereon/index.jsp). For primer sequences and amplified fragment sizes in Col and L*er*, see Table S1 in the supplementary material. For the list of sequencing primers, see Table S2 in the supplementary material.

RNA extraction and RT-PCR

Total RNA was isolated from 14-day-old wild-type and *chor* seedlings. cDNA synthesis and reverse-transcription (RT)-PCR were performed as described previously (Bemis and Torii, 2007), using the following primer pairs. For *CHOR* and *chor*, chorus cDNA F (5′-CAGCTTCATTAC-AATGCAATTCC-3′) and chorus cDNA R (5′-TCAAGTTACCAAA-ATATAGTCAACC-3′); for Actin control, ACT 2-1 (5′-GCCCATCCA-AGCTGTTCTCTC-3′) and ACT 2-2 (5′-GCTCGTAGTCAACAGCA-ACAA-3′); for sequencing RT-PCR products, chorus cDNA Seq F (5′-GCTCTACTGTTGATCATTTACA-3′).

Histochemical analysis and microscopy

Differential interference contrast (DIC) microscopy was performed according to Bemis and Torii (Bemis and Torii, 2007). For confocal microscopy, seedlings were treated with either propidium iodide (PI) or FM4-64 (Molecular Probes, Invitrogen). Fluorescence of GFP, YFP and PI/FM4-64 were simultaneously captured using a Zeiss LSM510 Meta or a Zeiss LSM700 (excitation, 488 nm and 543 nm; emission, 505-530 nm, 545-585 nm and 570-610 nm, respectively) with a 20× objective lens. For histochemical callose staining, seedlings were infiltrated with 0.1 mg/ml Aniline Blue fluorochrome (Biosupplies Australia) in 0.1% Silwett L77 (Lehle Seeds, Round Rock, TX) for 60 minutes and, prior to mounting, wild type and *chor* were counterstained briefly with FM4-64 to highlight the cell periphery. The abaxial side of rosette leaves was observed with a Zeiss LSM700 (excitation, 405 nm; emission, 475-500 nm). Aniline Blue-stained root hairs were observed with an Olympus BX51 epifluorescence microscope with a UV/B filter.

Quantitative analysis of stomatal phenotype

Twelve-day-old seedlings of wild type, *chor*, *er erl1* and *er erl1 chor* were subjected to DIC microscopy. Four non-overlapping frames of cotyledons, excluding the mid-vein region, and numbers of stomata and their cluster size were quantified using ImageJ.

Transient transformation of seedling leaf epidermis and cell-to-cell diffusion assay

Arabidopsis 10-day-old seedling rosette leaves were transiently transformed as previously described (Kanaoka et al., 2008). Briefly, microcarriers were prepared with 100 ng of plasmid containing *proCaMV35S::eCFP* (von Arnim et al., 1998), a combination of *proCaMV35S::eCFP* and *proCaMV35S::3xGFP* (J.S.L. and K.U.T., unpublished), or a combination of *proCaMV35S::eCFP* and *proCaMV35S::SPCH-YFP* (Lynn Pillitteri and K.U.T., unpublished). These plasmids were coated on 1.0-μm gold particles and bombarded using the PDS-1000/He particle delivery system (Bio-Rad, Hercules, CA, USA). Specimens were observed under a Zeiss LSM 510 Meta or an LSM700 confocal microscope. CFP, GFP or YFP fluorescence was monitored 6 hours after the bombardment.

Accession numbers

The GenBank Accession number for the GSL8 (CalS10) mRNA sequence is GQ373182.

RESULTS

chor, a stomatal patterning mutant obtained via a sensitized screen

We conducted a genetic screen using a sensitized *er erl1* background, in which two of the three *ER*-family genes are absent. *er erl1* plants develop an epidermis with an elevated stomatal density but are otherwise normal (Fig. 1) (Shpak et al., 2005). On rare occasions, paired stomata were observed both in wild-type and *er erl1* cotyledons (0.11% in wild type; 0.57% in *er*

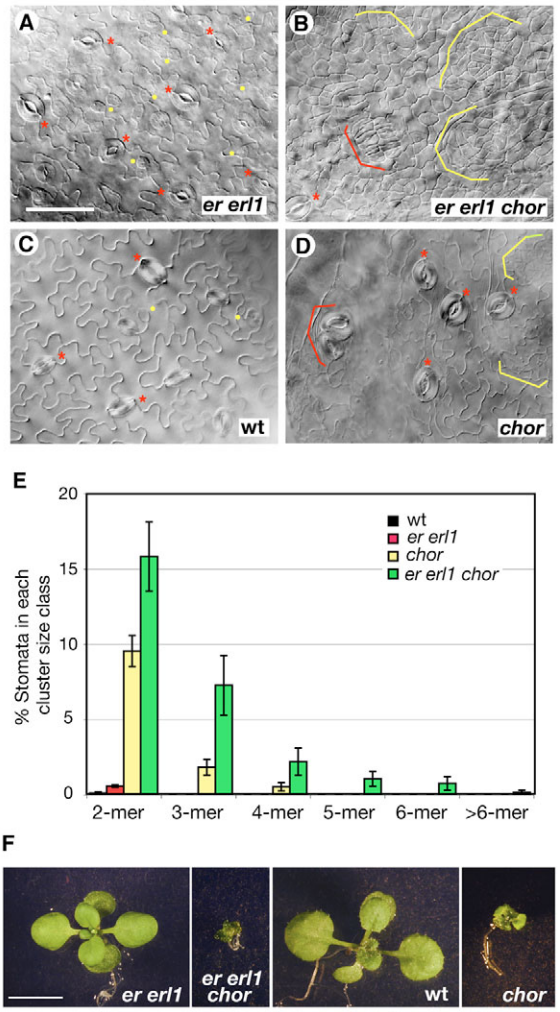

Fig. 1. *chor* mutant exhibits growth and stomatal patterning defects. (**A-D**) Abaxial rosette leaf epidermis from 2-week-old seedlings of *er erl1* (A), *er erl1 chor* (B), wild type (wt; C) and *chor* (D). *er erl1* produces a higher density of stomata (red asterisks) and stomatal precursors (yellow dots) than wild type, but it does not develop two stomata in contact (A,C). In *er erl1 chor*, aggregates of stomata (red bracket) and small, highly divided epidermal cells (yellow brackets) are visible (B). This phenotype is less prominent in *chor* (D). Images are taken under the same magnification. Scale bar: 50 μm. (**E**) Percentage of stomata in each cluster size class. Abaxial cotyledons from 12-day-old seedlings of wt, *er erl1*, *chor* and *er erl1 chor* were subjected to quantitative analysis. Average values are shown. Error bars indicate s.e.m. Number of seedlings analyzed: *n*=8, wt and *chor*; *n*=7, *er erl1* and *er erl1 chor*. Total number of stomata counted: wt, *n*=1771; *chor*, *n*=715; *er erl1*, *n*=1921; *er erl1 chor*, *n*=2721. (**F**) Representative 12-day-old plants of (from left to right) *er erl1*, *er erl1 chor*, wt, and *chor* in a wild-type background. Images are taken under the same magnification. Scale bar: 5 mm.

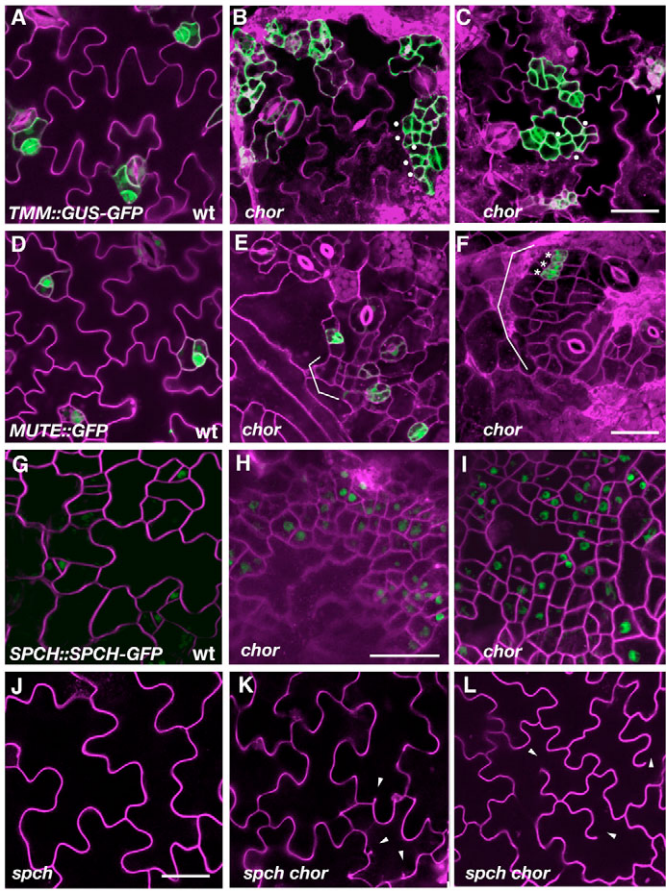

Fig. 2. *CHOR* is required to restrict stomatal cell-lineage divisions. (**A-C**) Promoter activity of *TMM* (proTMM::GUS-GFP) in 6-day-old cotyledon epidermis of wild type (A) and *chor* (B,C). In *chor,* clusters of small cells (dots) show high GFP signals. Pavement cells in *chor* occasionally show incomplete cytokinesis (arrowhead). (**D-F**) Expression of MUTE (proMUTE::MUTE-GFP) in 6-day-old cotyledon epidermis of wild type (D) and *chor* (E, F). Clusters of small stomatal-lineage cells are in brackets. *MUTE* expression in adjacent meristemoids (asterisks) predicts the eventual formation of clustered stomata. (**G-I**) Expression of SPCH (proSPCH::SPCH-GFP) in 3-day-old cotyledon epidermis of wild type (G) and *chor* (H, I). More cells express GFP signals in *chor* than in wild type. (**J-L**) Effects of *spch* on the excessive stomatal-lineage divisions in *chor*. Shown is 10-day-old cotyledon epidermis of *spch* (J) and *spch chor* (K,L). Small, highly divided cells are no longer produced in *spch chor* (K,L), whereas incomplete cytokinesis of pavement cells is still evident (K,L, arrowheads). Cell peripheries were highlighted by propidium iodide (PI; A-F,J-L) or FM4-64 (G-I). A-F, G-I, and J-L were taken under the same magnification. Scale bars: 20 μm.

erl1; Fig. 1E). Neither genotype developed stomatal clusters with three or more adjacent stomata (*n*=0/1771 and 0/1921 for wild type and *er erl1*, respectively; Fig. 1E). By contrast, *er erl1 erl2* triple loss-of-function mutants develop excessive numbers of clustered stomata (Shpak et al., 2005). We reasoned that in the absence of two of the three receptors, plants would be more sensitive to the loss of any additional regulators of stomatal patterning.

We isolated a line (#67). In the mutant leaves, multiple stomata are often formed in a compact aggregate with stomatal pairs (15.8%), trios (7.26%), quartets (2.19%), and 5-10 adjacent stomata (1.95%; Fig. 1B,E). In addition, aggregates of small epidermal cells, many resembling meristemoids, are formed in sectors across the epidermis (Fig. 1B). Segregation analysis showed that the mutation is recessive and monogenic (207:602, χ^2=0.149, *P*=0.700). The mutant was named *chorus* (*chor*) owing to its aggregated stomatal phenotype.

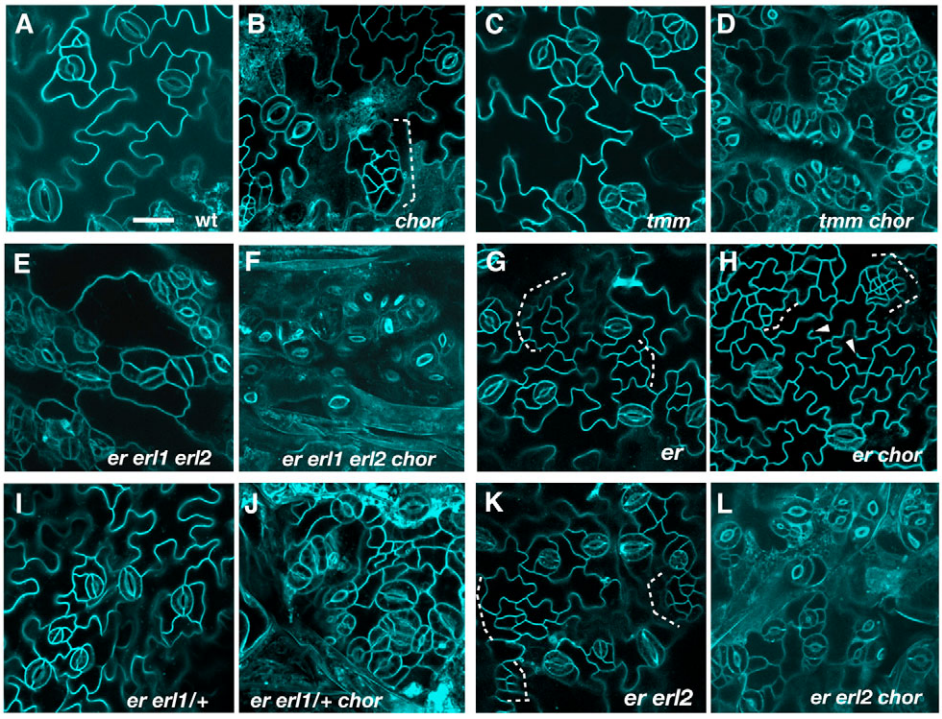

Fig. 3. Genetic interactions of *chor* with stomatal patterning mutants. (**A-L**) Abaxial epidermis of rosette leaves (first pairs) from 12-day-old seedlings of the following genotypes: wild type (wt, A), *chor* (B), *tmm* (C), *tmm chor* (D), *er erl1 erl2* (E), *er erl1 erl2 chor* (F), *er* (G), *er chor* (H), *er erl1/+* (I), *er erl1/+ chor* (J), *er erl2* (K) and *er erl2 chor* (L). *chor* in a wild-type background exhibits weak stomatal patterning defects and islands of small cells (dotted bracket; B), but the *chor* mutation severely enhances stomatal clustering in *tmm* (C,D) and in the *er erl1 erl2* triple mutant (E,F). *er erl1/+* and *er erl2* seedling leaves do not exhibit stomatal patterning defects (I,K); however, introduction of *chor* confers severe stomatal clustering defects (J,L). The *er chor* double-mutant phenotype appeared additive, with increased small cells (dotted bracket) and incomplete cytokinesis (arrowheads, G,H). Images are taken under the same magnification. Scale bar: 20 μm.

We introduced *chor* into the wild-type background to test whether the observed phenotype requires *er erl1*. The epidermal phenotype of *chor* leaves in the wild-type background was much milder than that of *chor er erl1*. Numbers of stomatal pairs (9.4%), trios (1.93%) and quartets (0.44%) were diminished. No stomatal clusters larger than quartets were found in *chor* (n=0/715; Fig. 1D,E). Similarly, fewer small epidermal cells were observed (Fig. 1D). Thus, *chor* phenotypes are enhanced by the loss of function in *ER* and *ERL1*. *chor* seedlings showed pleiotropic phenotypes, including severe dwarfism, short roots with disrupted cell files, short and branched root hairs, and seedling lethality (Fig. 1F; see also Figs S1 and S2 in the supplementary material). Furthermore, incomplete cytokinesis was frequently observed in *chor* (see Fig. S3 in the supplementary material). These findings suggest that *CHOR* is required for proper cell division and tissue patterning throughout plant organs, including stomatal patterning.

CHOR is required for restricting initiation and divisions of stomatal-lineage cells, as well as cytokinesis of epidermal cells

The *chor* leaf epidermis exhibited incomplete cytokinesis and excessive epidermal cell proliferation (Fig. 1). We hypothesized that the latter defect is due to excessive entry into the stomatal lineage. To test this, we examined the expression patterns of stomatal-lineage markers in *chor*. *TMM* marks early stomatal-lineage cells, including MMCs, meristemoids and SLGCs (Fig. 2A). Clusters of small, highly divided epidermal cells in *chor* seedlings exhibited high reporter activity of *proTMM::GUS-GFP* (Fig. 2B,C), suggesting that the *chor* mutation causes a vast increase in stomatal lineage divisions in a disorganized manner. *MUTE* is specifically expressed in late meristemoids that are differentiating into GMC (Fig. 2D) (Pillitteri et al., 2008; Pillitteri et al., 2007). Occasionally, multiple adjacent cells showed high *MUTE* promoter activity (Fig. 2F, asterisks), which is likely to predict the eventual formation of stomatal clusters.

The excessive formation of small stomatal-lineage cells is a hallmark of *SPCH* overexpression (MacAlister et al., 2007; Pillitteri et al., 2007). We therefore tested whether *SPCH* is ectopically expressed in *chor*, and whether *SPCH* is required for the *chor* epidermal phenotype. *SPCH* was expressed in early stomatal-lineage cells (Fig. 2G), and the *spch* mutant was devoid of stomatal cell lineages (Fig. 2J). Numerous SPCH-positive cells were observed in the young cotyledon epidermis of *chor* (Fig. 2H,I). Introduction of *spch* into *chor* eliminated all small, stomatal-lineage cells (Fig. 2K,L). By contrast, incomplete cytokinesis of pavement cells still occurred in the *chor spch* double mutant (Fig. 2K,L, arrowheads). These findings point to two independent roles of *CHOR* in regulating leaf epidermal development: *SPCH*-mediated initiation and division of stomatal cell lineage; and *SPCH*-independent cytokinesis. In support of this idea, the root epidermis of *spch chor* exhibited disrupted cell files with incomplete cytokinesis (see Fig. S1 in the supplementary material).

chor mutation exaggerates stomatal patterning defects and confers a breakdown of redundancy among cell-cell signaling components

The stomatal clustering phenotype of *chor* in the wild-type background remained relatively mild (Fig. 1). Therefore, the TMM/ER-family signaling pathway might still be able to largely enforce stomatal spacing in *chor*. To test this, we investigated the genetic interactions of *CHOR* with *TMM* and *ER*-family genes (Fig. 3). Quantitative analysis of stomatal cluster size was performed for key genotypes (see Fig. S4 in the supplementary material). In *tmm*, adjacent stomata are formed (Fig. 3C) (Nadeau and Sack, 2002a). The *tmm chor* double mutant developed massive clusters of stomata far more severe than those in either the *tmm* or the *chor* single mutant (Fig. 3B-D; see also Fig. S4 in the supplementary material). Similarly, the *chor* mutation intensified the stomatal cluster phenotype of the *er erl1 erl2* triple mutant (Fig. 3E,F).

We sought to understand whether *CHOR* acts in an independent pathway from (i.e. additive interaction) or an overlapping pathway with (i.e. synergistic interaction) the TMM/ER family. For this purpose, we genetically dissected the contribution of each *ER*-family member. The three *ER*-family genes exhibit unequal redundancy, and a stomatal cluster phenotype is manifested only when the entire family is lost (Figs 1, 3) (Shpak et al., 2005). *er* single mutants occasionally produce SLGCs that do not accompany differentiated stomata (Fig. 3G, dotted lines) (Shpak et al., 2005). The *er chor* epidermis formed severely divided patches of small cells (Fig. 3H, dotted brackets), but otherwise appeared similar to that of *chor* (Fig. 3H, arrowheads), thereby suggesting additive effects.

In contrast to *er chor*, *er erl1 chor* and *er erl2 chor* triple mutants exhibited severe stomatal clustering phenotypes (Fig. 1B; Fig. 3H,L; see also Fig. S4 in the supplementary material). We further tested whether such synergistic effects can be observed even when only a single copy of *ERL1* is eliminated. Indeed, *er erl1/+ chor* also showed a strong stomatal clustering phenotype (Fig. 3J). We conclude that *chor* intensifies stomatal cell-cell signaling defects and breaks down the functional redundancies among *ER*-family genes, with sensitivity to the dosage of *ERL*s.

Identification of *CHORUS* as *GLUCAN SYNTHASE LIKE 8*

To understand the molecular nature of *CHOR*, we performed map-based cloning. Our fine mapping delineated the *CHOR* locus within a 145-kb interval on chromosome 2 (Fig. 4A). Sequencing the interval led to the identification of a single G-to-A substitution at position 13447 of At2g36850, which encodes a putative callose synthase, *GSL8* (*CALS10*) (Fig. 4B). Because the original *chor* mapping population contained a mixed genome of Col/WS and L*er*, wild-type *GSL8* alleles from WS and L*er* were also sequenced. Both alleles possess G at this position, confirming that *CHOR* is not a naturally occurring polymorphism.

Sequence analysis of the wild-type *GSL8* transcripts revealed mis-annotation of *GSL8* in the existing database (see Materials and methods). Based on the experimental data, *GSL8* is a large gene consisting of 50 exons with a coding region of 5712 bp (GenBank Accession number GQ373182). In *chor*, the G-to-A substitution disrupted the splice acceptor site at intron 46 (Fig. 4B), which resulted in three major splicing variants (Fig. 4C). Variant 1 adopted the AG at +1 created by the *chor* G-to-A substitution and was one base pair shorter than the *CHOR* mRNA (see Fig. S5 in the supplementary material). Variants 2 and 3 were 60 and 130 bp longer than the *CHOR* mRNA, respectively. Variant 2 was produced by a cryptic splice acceptor site at –60 bp from the correct splicing acceptor site, whereas variant 3 was unspliced (see Fig. S5 in the supplementary material). All splicing variants caused frameshifts, each of which truncated the coding sequence starting from exon 47 and added instead a short stretch of 19, 10 and 16 out-of-frame amino acids, respectively (see Fig. S5 in the supplementary material).

GSL8 encodes a large integral membrane protein of 1905 amino acids with sixteen predicted transmembrane helices. The three splicing variants all result in truncation at the sixth extracytoplasmic hydrophilic loop and removal of five C-terminal transmembrane helices (Fig. 4D). To confirm that *CHOR* is *GSL8*, we characterized the phenotype of the available *GSL8* T-DNA insertion allele, *gsl8-2* (Toller et al., 2008; Chen et al., 2009). It was originally reported that *gsl8* confers male gametophytic lethality (Toller et al., 2008). However, data obtained by us and recently reported by other groups (Chen et al., 2009; Thiele et al., 2009) show that *gsl8* mutations result in seedling lethality with severe dwarfism (see Fig. S6 in the supplementary material). Cotyledons and leaves of *gsl8-2* plants exhibited similar stomatal patterning defects to those in *chor*, indicating that the *chor* phenotypes are due to loss of function in *GSL8* (Fig. 4E; data not shown). The fact that the degree of stomatal clustering was less severe in *chor* than in *gsl8-2* (Fig. 4E) suggests that *chor* might represent a partial loss-of-function allele. *GSL8* is expressed broadly throughout plant organs/tissues, based on the available expression data (Winter et al., 2007).

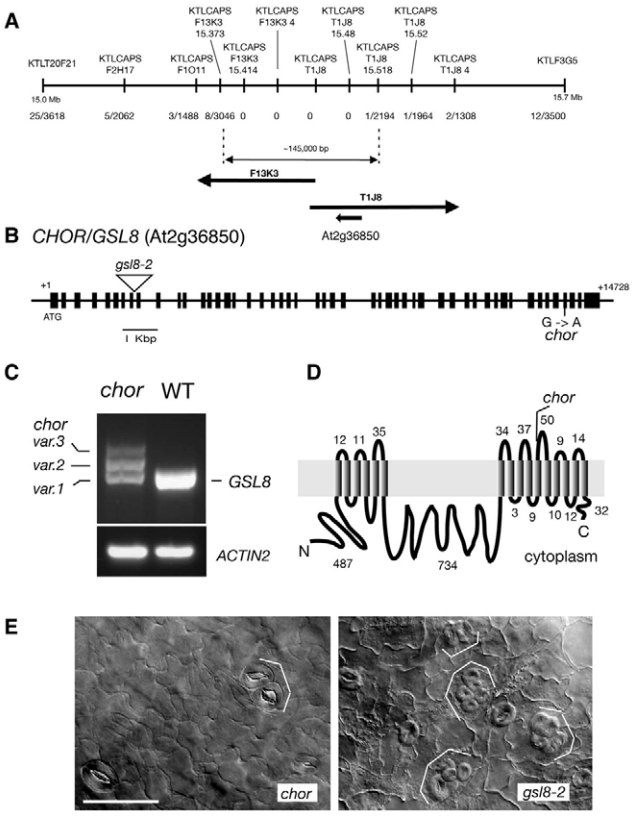

Fig. 4. Map-based cloning of *CHOR* as *GSL8*. (**A**) Physical mapping around the *CHOR* locus. The locations of molecular markers, the number of recombinants, and the corresponding BAC clone are indicated. The 145-kb interval and the position of the *CHOR* locus (At2g36850) are indicated as a double-headed arrow and a broad arrow, respectively. (**B**) *CHOR* (*GSL8*) gene structure. Boxes indicate exons; lines, introns. In *chor*, the G-to-A substitution occurred at the splice acceptor site on intron 46. (**C**) RT-PCR analysis of *chor* reveals the presence of three splicing variants (1363, 1293 and 1232 bp; see Materials and methods), none of which corresponds to the size of wild type (1233 bp). (**D**) Topology of the GSL8 protein. The GSL8 protein possesses 16 transmembrane helices. The *chor* mutation results in a truncation of the last three transmembrane helices and the C-terminal cytoplasmic tail. (**E**) Stomatal patterning defects of *gsl8-2*. Shown is adaxial cotyledon epidermis of 12-day-old *chor* (left) and *gsl8-2* (right). *gsl8-2* has aggregations of many more stomata than those seen in *chor* (brackets). Scale bar: 50 μm.

Both cell-plate and plasmodesmatal callose depositions are diminished in the developing *chor* leaf epidermis

Callose, a linear 1,3-β-glucan polymer, accumulates in various tissues/cells/organelles during normal development (Stone and Clarke, 1992). The incomplete cytokinesis observed in *chor* pavement

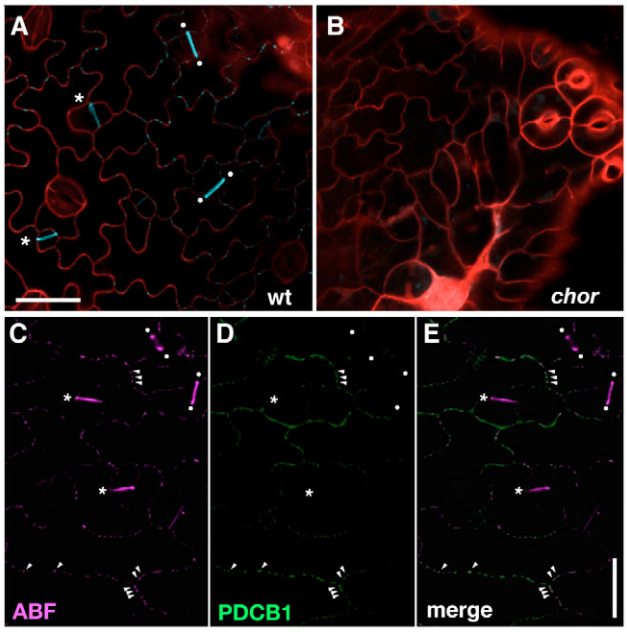

Fig. 5. Reduction in cell-plate, cell-wall and plasmodesmatal callose deposition in *chor* seedling epidermis. (**A**) Abaxial rosette leaf epidermis of a 2-week-old wild-type seedling. Callose deposition is notable at the cell plates of newly divided meristemoids (asterisks) and GMC (dots). Strong punctate signals, characteristic of plasmodesmatal callose deposition, are detected at the cell periphery. (**B**) Abaxial rosette leaf epidermis of a 12-day-old *chor* seedling under the same callose staining treatment as the seedling in A. FM4-64 was used to highlight the cell periphery. (**C-E**) Colocalization (e.g. arrowheads) of a plasmodesmata marker YFP-PDCB1 (D, green) and callose staining (C, magenta) supporting the identity of the fluorescent punctae. Merged images are shown in E. Note that callose depositions at the cell plates (asterisks) and ventral cell walls of stomata (dots) do not co-localize with YFP-PDCB1. Images are taken under the same magnification. Scale bars: 20 μm.

cells (see Fig. S3 in the supplementary material) is consistent with the recent finding that GSL8 acts as a cell-plate callose synthase (Thiele et al., 2009). In addition to its role in the cell plate, callose deposition imposes physical constraints to the symplastic channel (Levy et al., 2007b; Radford et al., 1998). To address the role of GSL8 during stomatal development, we examined callose deposition in wild-type and *chor* seedlings using a callose-specific dye, Aniline Blue fluorochrome (Fig. 5) (Stone et al., 1984). In the wild-type rosette leaf epidermis, bright, linear signals marked cell plates in dividing cells (Fig. 5A, asterisks and dots). In addition, strong, punctate fluorescent signals were detected on the walls of epidermal cells, most notably in pavement cells and SLGCs (Fig. 5A), which is characteristic of plasmodesmatal callose deposition (Levy et al., 2007a; Simpson et al., 2009). Consistently, these punctate signals co-localized with the plasmodesmatal marker YFP-PDCB1 (Fig. 5E) (Simpson et al., 2009).

In contrast to the wild type, almost no Aniline Blue signals were detected in the *chor* leaf epidermis (Fig. 5B). We also noted the absence of callose deposition in *chor* root hairs and abnormal root hair morphology (see Fig. S2 in the supplementary material). On the basis of these findings, we conclude that *GSL8* is required for the proper accumulation of callose at cell plates, cell walls and plasmodesmata.

Loss of *CHOR* (*GSL8*) causes relaxation of cell-to-cell connection in the epidermis

Because GSL8 is required for both cell-plate and plasmodesmatal callose deposition (Fig. 5), we postulated that the overproliferation of stomatal-lineage cells might be due to the reduction in plasmodesmatal callose deposition. As a first step towards gaining mechanistic insight, we investigated whether symplastic cell-to-cell connections are altered in the *chor* epidermis. Monomeric soluble CFP was used as a reporter to monitor passive diffusion from cell to cell. Specifically, CaMV35S::CFP was bombarded to the leaf epidermis, and diffusion of CFP signals from the point of initial CFP expression was assayed. A similar method has been recently used to assess cell-to-cell trafficking (Levy et al., 2007a; Simpson et al., 2009). In nearly all cases in wild type (n=19/21), a single cell at the site of transformation showed a bright CFP signal (Fig. 6; see also Fig. S7 in the supplementary material). A few surrounding cells showed a dim CFP signal, indicating diffusion (Fig. 6; see Fig. S7 in the supplementary material). *chor* epidermal cells without obvious cytokinesis defects were examined in diffusion assays. An average of four to five adjacent cells in the *chor* epidermis showed strong CFP fluorescence with many more surrounding cells showing dim CFP signals (Fig. 6; see Fig. S7 in the supplementary material). Total numbers of CFP-expressing cells per site in the *chor* epidermis (16.8±2.68, mean ± s.e.m.) were significantly higher than those in the wild-type epidermis (5.7±1.24; P<0.0006).

To address whether the size exclusion limit (SEL) was increased in *chor*, we simultaneously introduced trimeric GFP (3×GFP) and control CFP via co-bombardment and monitored their diffusion (Fig. 6). In wild type, all cells expressing 3×GFP (n=22/22) were solitary (Fig. 6A,C). Thus, unlike with CFP (Fig. 6A,B), there was no diffusion of 3×GFP, indicating that 3×GFP is beyond the SEL in the wild-type epidermis. By contrast, in the *chor* epidermis, a cluster of epidermal cells expressed 3×GFP (Fig. 6A,C). In some cases, a cell adjacent to the site of transformation exhibited a dim GFP signal (Fig. 6A, asterisk), indicating that 3×GFP was able to spread into neighboring cells in the *chor* epidermis. These results suggest that the reduced plasmodesmatal callose deposition caused by the *chor* mutation is associated with an increase in symplastic connectivity between leaf epidermal cells.

chor mutation allows cell-to-cell movement of SPCH-YFP in the leaf epidermis

In *chor*, SPCH-mediated stomatal cell-lineage divisions become excessive and dysregulated (Fig. 2). To explore the mechanistic link between increased cell-to-cell connections and stomatal patterning, we tested the diffusion of functional SPCH-YFP in wild-type and *chor* epidermis. For this purpose, SPCH-YFP and control CFP constructs were co-bombarded (Fig. 7). In wild type, YFP signal was detected solely in the nucleus of a single cell at the site of transformation (n=20/20; Fig. 7A,C), indicating that SPCH-YFP does not diffuse from cell to cell. By contrast, in *chor* epidermis multiple adjacent cells expressed SPCH-YFP (Fig. 7A,C). In some cases, neighboring cells exhibited a dim YFP signal in the nucleus (Fig. 7A, asterisk). The presence of a continuous cell periphery indicates that these YFP-positive nuclei are not likely from a single multinucleate cell. The results demonstrate that SPCH-YFP diffuses from cell-to-cell in the *chor* epidermis and suggests that the failure to properly contain cell-fate determinants in *chor* causes the stomatal patterning defects.

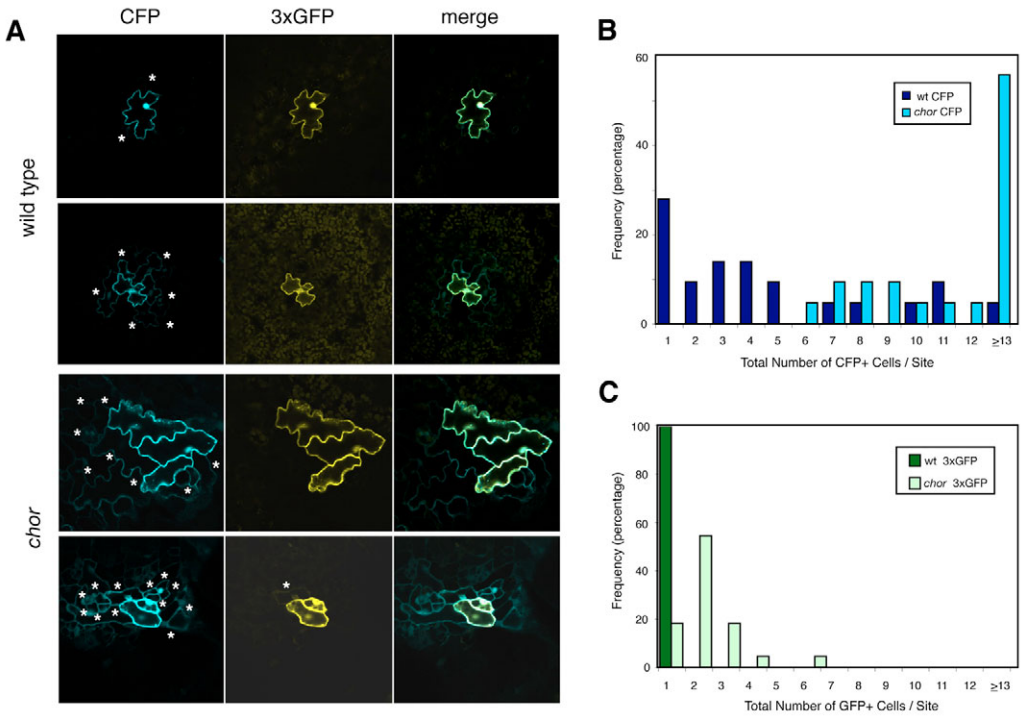

Fig. 6. Increased cell-to-cell macromolecular diffusion in *chor*. (**A**) Representative images of 10-day-old wild-type (top) and *chor* (bottom) epidermis expressing co-bombarded monomeric CFP (cyan, left) and trimeric GFP (yellow, middle). Merged images are shown on the right. Bright signals are detected at the site of transformation. Dim signals in surrounding neighbors (asterisks) indicate diffusion. Images are taken under the same magnification. (**B**,**C**) Quantitative distribution analysis of the number of cells expressing CFP (B) or 3×GFP (C) per site. Only continuous clusters of cells surrounding a cell (or cells) co-expressing strong CFP/GFP signals, which imply a single transformation event, were considered as a site (*n*=22, wild type and *chor*).

Epidermal phenotypes and symplastic connectivity in cytokinesis-defective mutants

Because *GSL8* is required for cytokinesis, incomplete cell division within the epidermis might also contribute to the dysregulated partitioning of regulatory macromolecules. To clarify this, we examined the epidermal phenotype and cell-to-cell connectivity in two well-described cytokinesis mutants, *atnack1* (*hinkel*) (Nishihama et al., 2002; Strompen et al., 2002) and *scd1* (*stomatal cytokinesis-defective 1*) (Falbel et al., 2003). Like *chor*, *atnack1* and *scd1* seedlings exhibit dwarfism but produce rosette leaves and survive for 2-3 weeks after germination (data not shown).

Consistent with the previous descriptions in tobacco leaves (Nishihama et al., 2002), cotyledon and rosette leaf epidermis of *atnack1* showed occasional incomplete cytokinesis of pavement cells (Fig. 8A, arrowheads) and GMCs (Fig. 8A, asterisks), the latter of which resulted in abnormal stomata with incomplete separation of the guard cells. As reported previously (Falbel et al., 2003), incomplete cytokinesis and reduced lobing of pavement cells are also observed in the *scd1* epidermis (Fig. 8A, plus signs). *scd1* GMCs failed to divide and expand (Fig. 8A). In spite of these defects, neither *atnack1* nor *scd1* epidermis showed excessive production of stomatal-lineage cells or severe stomatal clusters (Fig. 8A), indicating that stomatal patterning phenotypes in *chor* are not simply due to defective cytokinesis.

Next we investigated cell-to-cell diffusion of SPCH-YFP and soluble CFP in *atnack1* and *scd1* leaf epidermis (Fig. 8B-D), and compared the results with wild type and *chor* (Fig. 7). Among the four genotypes, only *chor* exhibited a significant difference in CFP diffusion (Tukey's HSD test with ANOVA, $P<0.01$). As in wild type, SPCH-YFP was detected solely in the nucleus of a single cell at the site of transformation in *atnack1* (*n*=16/16) and *scd1* (*n*=20/20; Fig. 8B,D). The results are inconsistent with the hypothesis that leakiness of cells is a common consequence of incomplete cytokinesis.

DISCUSSION

From a sensitized genetic screen, we have identified *CHOR*, which is required for organized initiation of the stomatal cell lineage and proper stomatal patterns. The molecular identity of CHOR as a putative callose synthase, GSL8, and seedling callose staining data demonstrate that *GSL8* is required for cell-plate and plasmodesmatal callose deposition. A series of cell-to-cell diffusion assays illuminates the link between altered symplastic connectivity and stomatal fate specification.

Among the twelve putative callose synthase genes [*GSLs* (*CalSs*)] (Hong et al., 2001), *GSL1* (*CalS11*), *GSL5* (*CalS12*), *GSL2* (*CalS5*), *GSL8* (*CalS10*) and *GSL10* (*CalS9*) have been shown to be required for microgametogenesis and pollen development (Dong et al., 2005; Enns et al., 2005; Nishikawa et al., 2005; Toller et al., 2008). Recent reverse-genetic studies by Chen et al. showed that most *gsl* mutants exhibited a nearly normal seedling growth phenotype (Chen et al., 2009), suggesting that many callose synthase genes act redundantly during sporophytic development. Our findings extend the recent reports (Chen et al., 2009; Thiele et al., 2009), and reveal roles of GSL8 in addition to its role in cytokinesis. Swollen, branched root hairs in *chor* and *gsl8-2* (see Fig. S2 in the supplementary material)

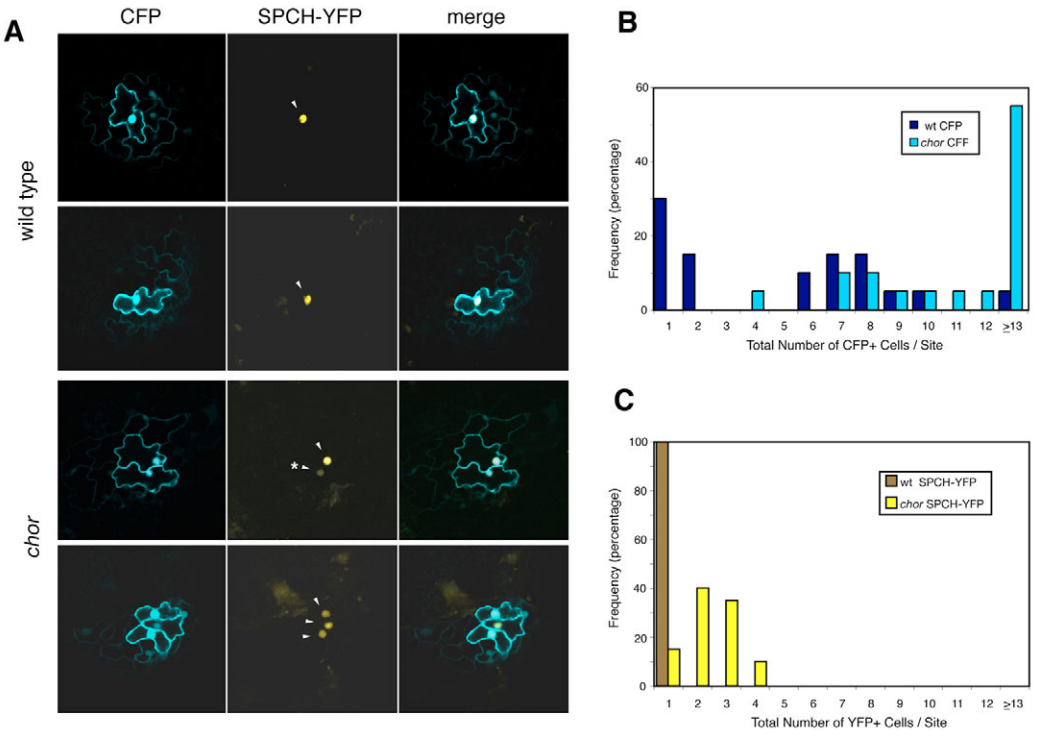

Fig. 7. Cell-to-cell diffusion of SPCH-YFP in *chor*. (**A**) Representative images of 10-day-old wild-type (top) and *chor* (bottom) epidermis expressing co-bombarded monomeric CFP (cyan, left) and SPCH-YFP (yellow, middle). Merged images are shown on the right. SPCH-YFP was detected solely in the nuclei (arrowheads). Dim YFP signals in neighboring nuclei (asterisks) indicate diffusion. Images are taken under the same magnification. (**B**,**C**) Quantitative distribution analysis of the number of cells expressing CFP (B) or SPCH-YFP (C) per site. In wild type, SPCH-YFP was only detected in one cell/site (*n*=20, wild type and *chor*).

indicate that root-hair callose is necessary for proper root-hair-cell polarity and morphogenesis. Thiele et al. (Thiele et al., 2009) reported that seedlings of *massue*, which is allelic to *chor*, exhibit normal root-hair morphology. The difference between our observations and those of Thiele et al. (Thiele et al., 2009) might be due to specific growth conditions, such as a difference in mineral ion concentrations in the growth media, which affect root hair morphology and patterning (Muller and Schmidt, 2004; Yang et al., 2008).

Callose turnover at the plasmodesmata is likely to be determined by an intricate balance of callose synthase- and β-1,3 glucanase activities. Recent proteomic analyses of plasmodesmatal proteins led to the identification of a β-1,3 glucanase, AtBG_ppap (Levy et al., 2007a), as well as of GPI-anchored plasmodesmatal neck proteins that anchor callose via direct binding (Simpson et al., 2009). A loss-of-function mutation in AtBG_ppap conferred increased plasmodesmatal callose deposition and reduced cell-to-cell diffusion of free GFP (Levy et al., 2007a), a phenotype that is opposite to that of *chor*.

The fact that GSL8 is required for both cell-plate and plasmodesmatal callose deposition complicates the interpretation of *chor* epidermal phenotypes, as incomplete cytokinesis could also contribute to cell leakiness. Our cell-to-cell diffusion assays using *atnack1* and *scd1* demonstrate that this is not likely to be the case. *AtNACK1* encodes a kinesin-related protein that is required for cell-plate expansion (Nishihama et al., 2002; Strompen et al., 2002). *SCD1* encodes a protein with a DENN domain and WD-40 repeats, which is implicated in the trafficking of secretory vesicles during cell-plate formation and polar cell growth (Falbel et al., 2003). Although *atnack1* and *scd1* produced aberrant stomata with incomplete GMC divisions, neither mutant showed overproliferation of stomatal-lineage cells or severe stomatal clusters. Thus, the overproduction of stomatal-lineage cells in *chor* is likely to be a consequence of reduced plasmodesmatal callose deposition.

chor conferred massive stomatal cluster formation in plants lacking TMM or partially lacking members of the ER family (Figs 1, 3), suggesting that *CHOR* is required for full manifestation of inhibitory signaling via TMM and the ER family. How do cell leakiness and loss/reduction in a transmembrane signaling system together result in severe stomatal cluster formation? We propose the following model based on our findings (Fig. 9). In wild type, stomatal cell-fate determinants are tightly contained in stomatal initials (i.e. MMC) and precursors (i.e. meristemoids). Inhibitory signals, such as EPF peptides, further prevent the neighboring cells form adopting a stomatal-lineage fate (Fig. 9A). In the absence of *CHOR*, cell-fate determinants leak from the stomatal initials/precursors to their neighbors, causing excessive entry divisions. However, functional TMM/ER-family signaling can target these cell-fate determinants and enforce stomatal patterning to some extent (Fig. 9B). The loss of CHOR in combination with the loss of TMM/ER-family signaling (or with even a slight reduction in signaling, such as a heterozygous loss of *ERL1* in *er chor*) results in catastrophic and excessive stomatal differentiation (Fig. 9C).

Several lines of evidence support the hypothesis that SPCH might be such a cell-fate determinant. First, excessive entry into stomatal cell lineages, as seen in *chor,* is characteristic of *SPCH* overexpression. Second, *spch* loss-of-function mutation eliminates

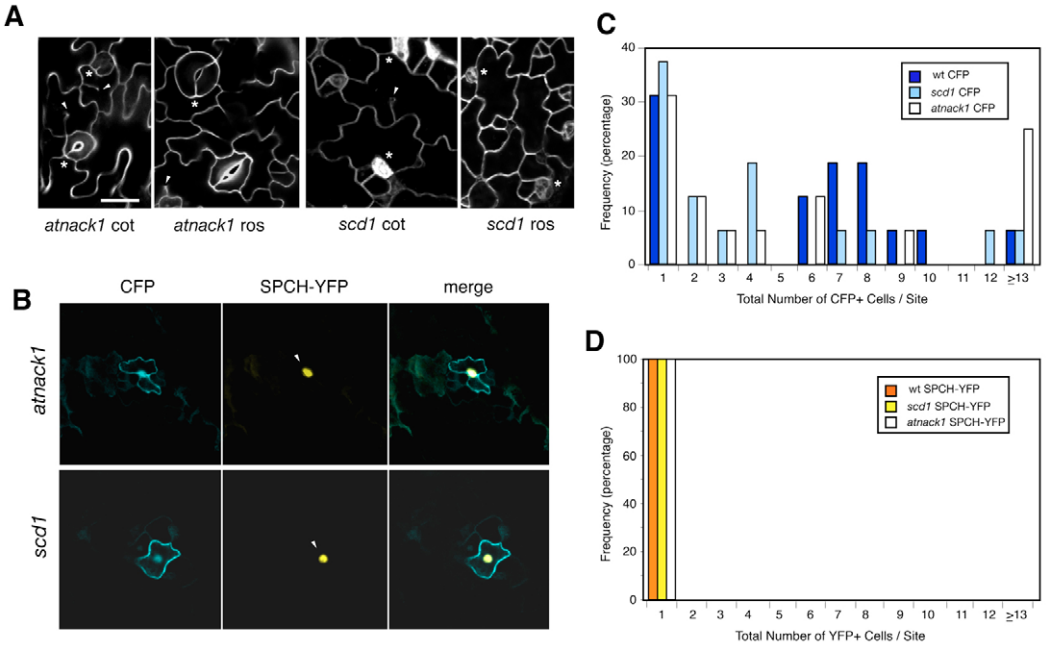

Fig. 8. Epidermal phenotypes and cell-to-cell diffusion assays in two cytokinesis mutants, *atnack1* and *scd1*. (**A**) Shown are cotyledon and rosette leaf epidermis of 10-day-old *atnack1* (left) and *scd1* (right) seedlings. Both mutants exhibit occasional cytokinesis defects in pavement cells (arrowheads) and stomata (asterisks), but otherwise do not show the stomatal patterning phenotype seen in *chor*. (**B**) *atnack1* (top) and *scd1* (bottom) epidermis expressing co-bombarded monomeric CFP (cyan, left) and SPCH-YFP (yellow, middle). Merged images are shown on the right. SPCH-YFP was detected solely in the nuclei (arrowheads) of solitary cells. Images are taken under the same magnification. (**C**,**D**) Quantitative distribution analysis of the number of cells expressing CFP (C) or SPCH-YFP (D) per site. SPCH-YFP was detected in only one cell/site (n=20, wild type and *scd1*; n=16, *atnack1*).

all of the small, highly divided cells in *chor* cotyledons and leaves, whereas incomplete cytokinesis defects in pavement cells remain unaffected. Third, more cells in the *chor* protoderm than in wild type express SPCH-GFP protein driven by its own promoter. Lastly, SPCH-YFP spreads from cell to cell in the *chor* epidermis. It has been proposed that the inhibitory cell-cell signal mediated via TMM/ER-family receptors targets and inhibits SPCH activity via YODA-dependent phosphorylation (Lampard et al., 2008). In this regard, it is worth mentioning that the expression of a phosphorylation-resistant version of SPCH also conferred a breakdown of redundancy among *ER*-family genes (Lampard et al., 2008).

ERLs were more sensitive than ER to the effects of *chor* (see Fig. 3; see Fig. S4 in the supplementary material). This further supports our hypothesis that *SPCH* activity becomes excessive and dysregulated in *chor*. *ER* and *ERLs* have redundant yet unique roles during stomatal development. *ER* is expressed throughout protodermal tissues, while *ERLs* are specifically expressed in stomatal-lineage cells (meristemoids and SLGCs) (Shpak et al., 2005). Consistently, ERLs inhibit the differentiation of meristemoids, while ER only has an earlier role (Shpak et al., 2005). It is possible that while the TMM/ER-family-mediated signaling pathway targets SPCH, SPCH in turn promotes the expression and hence the function of ERLs.

Our studies reveal an exciting link between the regulation of intracellular macromolecule trafficking and stomatal patterning. Selective trafficking of regulatory molecules, such as transcription factors and small RNAs, influences cell-fate specification in plants, such as root tissue patterning and coordinated growth within the shoot apical meristem (Lucas and Lee, 2004; Oparka and Roberts, 2001). Thus far, intercellular movements of key transcription factors have not been observed during stomatal development. Rather, all five key stomatal bHLH proteins are expressed solely in specific

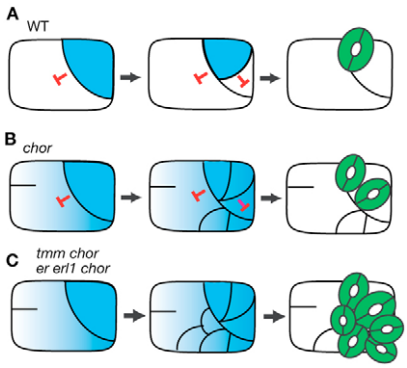

Fig. 9. Model of phenotypical consequences of the loss of *CHOR* (*GSL8*) and signaling receptors. (**A**) In wild type, stomatal cell-fate determinants (cyan) are contained in a precursor cell, and inhibitory signals (red T bar) prevent its neighbors from adopting a stomatal-lineage fate. (**B**) In *chor*, cell-fate determinants (cyan) may leak through plasmodesmata, which results in excessive stomatal entry divisions. The functional inhibitory signals, however, are able to prevent the stomatal differentiation of neighbors at some level. This results in modest stomatal clusters. Incomplete cytokinesis also occurs in *chor*. (**C**) In the absence of both CHOR (GSL8) and signaling receptors (such as TMM), the loss (or reduction at the threshold level in *er erl1*) of inhibitory signals together with the leakage of cell-fate determinants leads to catastrophic stomatal patterning defects.

stomatal precursors (SPCH, MUTE and FAMA), or in stomatal precursors throughout stomatal development (SCRM and SCRM2), but not in their neighbors, consistent with their intrinsic, cell-autonomous actions (MacAlister et al., 2007; Ohashi-Ito and Bergmann, 2006; Pillitteri et al., 2008; Pillitteri et al., 2007).

Owing to their nature as turgor-driven valves, mature guard cells constituting stomata are symplastically isolated and are consistently devoid of functional plasmodesmata (Willmer and Saxton, 1979). However, ultrastructural studies in some plant species have shown that developing stomatal precursors and their neighbors are connected via plasmodesmata (Kaufman et al., 1970; Willmer and Saxton, 1979). Imposing restrictions in cell-to-cell trafficking by callose deposition therefore could be a crucial means of segregating key cell-fate determinants while maintaining integrity between neighboring cells. In addition to regulatory proteins, movement of small RNAs might influence stomatal patterning. It has been reported that the microRNA miR824 and its target *AGL16* are localized in different cell types within stomatal cell lineages, and this observation led to the hypothesis that they might act non-cell autonomously via plasmodesmata to regulate satellite meristemoid divisions (Kutter et al., 2007). Future studies to determine the distribution and cell-to-cell trafficking of these regulators in *chor*, and a precise delineation of cytokinesis and the plasmodesmatal functions of CHOR (GSL8), might reveal the exact mechanism by which cell-to-cell trafficking enforces proper stomatal patterning.

Acknowledgements

We thank Lynn Pillitteri and Jennifer Nemhauser for comments; Lynn Pillitteri, Michiko Sasabe, Yasunori Machida, Sebastian Bednarek, Andrew Maule, and NASC for plasmids and mutants/transgenic lines; Bruce Godfrey for assisting particle bombardment; Greg Martin and Amanda Rychel for assisting confocal microsopy; Tetsuya Higashiyama and Narie Sasaki for providing facilities to M.M.K. This work was supported by NSF (IOB0744892), DOE (DE-FG02-03ER15448) and JST-PREST awards to K.U.T., NSF (MCB0548525 and IOB0543923) awards to Z.H., and Japan NEXT Grant-in-Aid for Young Scientists (Start-up:20870020 and B:21770041) to M.M.K. K.M.P. is an NSF graduate research fellow.

Competing interests statement

The authors declare no competing financial interests.

Supplementary material

Supplementary material for this article is available at
http://dev.biologists.org/lookup/suppl/doi:10.1242/dev.049197/-/DC1

References

Bemis, S. M. and Torii, K. U. (2007). Autonomy of cell proliferation and developmental programs during Arabidopsis aboveground organ morphogenesis. *Dev. Biol.* **304**, 367-381.

Bergmann, D. C. and Sack, F. D. (2007). Stomatal development. *Annu. Rev. Plant. Biol.* **58**, 163-181.

Bergmann, D. C., Lukowitz, W. and Somerville, C. R. (2004). Stomatal development and pattern controlled by a MAPKK kinase. *Science* **304**, 1494-1497.

Chen, X. Y., Liu, L., Lee, E., Han, X., Rim, Y., Chu, H., Kim, S. W., Sack, F. and Kim, J. Y. (2009). The Arabidopsis callose synthase gene *GSL8* is required for cytokinesis and cell patterning. *Plant Physiol.* **150**, 105-113.

Dievart, A. and Clark, S. E. (2004). LRR-containing receptors regulating plant development and defense. *Development* **131**, 251-261.

Dong, X., Hong, Z., Sivaramakrishnan, M., Mahfouz, M. and Verma, D. P. (2005). Callose synthase (CalS5) is required for exine formation during microgametogenesis and for pollen viability in Arabidopsis. *Plant J.* **42**, 315-328.

Enns, L. C., Kanaoka, M. M., Torii, K. U., Comai, L., Okada, K. and Cleland, R. E. (2005). Two callose synthases, GSL1 and GSL5, play an essential and redundant role in plant and pollen development and in fertility. *Plant Mol. Biol.* **58**, 333-349.

Falbel, T. G., Koch, L. M., Nadeau, J. A., Segui-Simarro, J. M., Sack, F. D. and Bednarek, S. Y. (2003). SCD1 is required for cytokinesis and polarized cell expansion in *Arabidopsis thaliana*. *Development* **130**, 4011-4024.

Hara, K., Kajita, R., Torii, K. U., Bergmann, D. C. and Kakimoto, T. (2007). The secretory peptide gene *EPF1* enforces the stomatal one-cell-spacing rule. *Genes Dev.* **21**, 1720-1725.

Hara, K., Yokoo, T., Kajita, R., Onishi, T., Yahata, S., Peterson, K. M., Torii, K. U. and Kakimoto, T. (2009). Epidermal cell density is auto-regulated via a secretory peptide, EPIDERMAL PATTERNING FACTOR2 in Arabidopsis leaves. *Plant Cell Physiol.* **50**, 1019-1031.

Hong, Z., Delauney, A. J. and Verma, D. P. (2001). A cell plate-specific callose synthase and its interaction with phragmoplastin. *Plant Cell* **13**, 755-768.

Hunt, L. and Gray, J. E. (2009). The signaling peptide EPF2 controls asymmetric cell divisions during stomatal development. *Curr. Biol.* **19**, 864-869.

Kanaoka, M. M., Pillitteri, L. J., Fujii, H., Yoshida, Y., Bogenschutz, N. L., Takabayashi, J., Zhu, J. K. and Torii, K. U. (2008). *SCREAM/ICE1* and *SCREAM2* specify three cell-state transitional steps leading to Arabidopsis stomatal differentiation. *Plant Cell* **20**, 1775-1785.

Kaufman, P. B., Petering, L. B., Yocum, C. S. and Baic, D. (1970). Ultrastructural studies on stomata development in internodes of Avena sativa. *Amer. J. Bot.* **57**, 33-49.

Kutter, C., Schob, H., Stadler, M., Meins, F., Jr and Si-Ammour, A. (2007). MicroRNA-mediated regulation of stomatal development in Arabidopsis. *Plant Cell* **19**, 2417-2429.

Lai, L. B., Nadeau, J. A., Lucas, J., Lee, E. K., Nakagawa, T., Zhao, L., Geisler, M. and Sack, F. D. (2005). The Arabidopsis R2R3 MYB proteins FOUR LIPS and MYB88 restrict divisions late in the stomatal cell lineage. *Plant Cell* **17**, 2754-2767.

Lampard, G. R., Macalister, C. A. and Bergmann, D. C. (2008). Arabidopsis stomatal initiation is controlled by MAPK-mediated regulation of the bHLH SPEECHLESS. *Science* **322**, 1113-1116.

Levy, A., Erlanger, M., Rosenthal, M. and Epel, B. L. (2007a). A plasmodesmata-associated beta-1,3-glucanase in Arabidopsis. *Plant J.* **49**, 669-682.

Levy, A., Guenoune-Gelbart, D. and Epel, B. (2007b). β-1,3 Glucanases-Plasmodesmatal gate keepers for intercellular communication. *Plant Signal. Behav.* **2**, 404-407.

Loudet, O., Chaillou, S., Camilleri, C., Bouchez, D. and Daniel-Vedele, F. (2002). Bay-0 x Shahdara recombinant inbred line population: a powerful tool for the genetic dissection of complex traits in Arabidopsis. *Theor. Appl. Genet.* **104**, 1173-1184.

Lucas, W. J. and Lee, J. Y. (2004). Plasmodesmata as a supracellular control network in plants. *Nat. Rev. Mol. Cell Biol.* **5**, 712-726.

Lukowitz, W., Gillmor, C. S. and Scheible, W. R. (2000). Positional cloning in Arabidopsis. Why it feels good to have a genome initiative working for you. *Plant Physiol.* **123**, 795-805.

Lukowitz, W., Roeder, A., Parmenter, D. and Somerville, C. (2004). A MAPKK kinase gene regulates extra-embryonic cell fate in Arabidopsis. *Cell* **116**, 109-119.

MacAlister, C. A., Ohashi-Ito, K. and Bergmann, D. C. (2007). Transcription factor control of asymmetric cell divisions that establish the stomatal lineage. *Nature* **445**, 537-540.

Muller, M. and Schmidt, W. (2004). Environmentally induced plasticity of root hair development in Arabidopsis. *Plant Physiol.* **134**, 409-419.

Nadeau, J. A. and Sack, F. D. (2002a). Control of stomatal distribution on the Arabidopsis leaf surface. *Science* **296**, 1697-1700.

Nadeau, J. A. and Sack, F. D. (2002b). Stomatal Development in Arabidopsis. Rockville, MD: American Society of Plant Biologists. doi: 10.1199/tab.0066 http://www.aspb.org/publications/arabidopsis/.

Neff, M. M., Neff, J. D., Chory, J. and Pepper, A. E. (1998). dCAPS, a simple technique for the genetic analysis of single nucleotide polymorphisms: experimental applications in Arabidopsis thaliana genetics. *Plant J.* **14**, 387-392.

Nishihama, R., Soyano, T., Ishikawa, M., Araki, S., Tanaka, H., Asada, T., Irie, K., Ito, M., Terada, M., Banno, H. et al. (2002). Expansion of the cell plate in plant cytokinesis requires a kinesin-like protein/MAPKKK complex. *Cell* **109**, 87-99.

Nishikawa, S., Zinkl, G. M., Swanson, R. J., Maruyama, D. and Preuss, D. (2005). Callose (beta-1,3 glucan) is essential for Arabidopsis pollen wall patterning, but not tube growth. *BMC Plant Biol.* **5**, 22.

Ohashi-Ito, K. and Bergmann, D. C. (2006). Arabidopsis *FAMA* controls the final proliferation/differentiation switch during stomatal development. *Plant Cell* **18**, 2493-2505.

Oparka, K. J. and Roberts, A. G. (2001). Plasmodesmata. A not so open-and-shut case. *Plant Physiol.* **125**, 123-126.

Pillitteri, L. J., Sloan, D. B., Bogenschutz, N. L. and Torii, K. U. (2007). Termination of asymmetric cell division and differentiation of stomata. *Nature* **445**, 501-505.

Pillitteri, L. J., Bogenschutz, N. L. and Torii, K. U. (2008). The bHLH protein, MUTE, controls differentiation of stomata and the hydathode pore in Arabidopsis. *Plant Cell Physiol.* **49**, 934-943.

Radford, J. E., Vesk, M. and Overall, R. L. (1998). Callose deposition at plasmodesmata. *Protoplasma* **201**, 30-37.

Shiu, S. H. and Bleecker, A. B. (2001). Plant receptor-like kinase gene family: diversity, function, and signaling. *Sci. STKE* **2001**, RE22.
Shpak, E. D., Berthiaume, C. T., Hill, E. J. and Torii, K. U. (2004). Synergistic interaction of three ERECTA-family receptor-like kinases controls Arabidopsis organ growth and flower development by promoting cell proliferation. *Development* **131**, 1491-1501.
Shpak, E. D., McAbee, J. M., Pillitteri, L. J. and Torii, K. U. (2005). Stomatal patterning and differentiation by synergistic interactions of receptor kinases. *Science* **309**, 290-293.
Simpson, C., Thomas, C., Findlay, K., Bayer, E. and Maule, A. J. (2009). An Arabidopsis GPI-anchor plasmodesmal neck protein with callose binding activity and potential to regulate cell-to-cell trafficking. *Plant Cell* **21**, 581-594.
Stone, B. A. and Clarke, A. E. (1992). Chemistry and physiology of higher plant 1,3-β-glucans (callose). In *Chemistry and Biology of (1,3) β-glucans* (ed. B. A. Stone and A. E. Clarke), pp. 365-429. Bundoora, Australia: La Trobe University Press.
Stone, B. A., Evans, N. A., Bonig, I. and Clarke, A. E. (1984). The application of Sirofluor, a chemically defined fluorochrome from aniline blue for the histochemical detection of callose. *Protoplasma* **122**, 191-195.
Strompen, G., El Kasmi, F., Richter, S., Lukowitz, W., Assaad, F. F., Jurgens, G. and Mayer, U. (2002). The Arabidopsis HINKEL gene encodes a kinesin-related protein involved in cytokinesis and is expressed in a cell cycle-dependent manner. *Curr. Biol.* **12**, 153-158.
Thiele, K., Wanner, G., Kindzierski, V., Jurgens, G., Mayer, U., Pachl, F. and Assaad, F. F. (2009). The timely deposition of callose is essential for cytokinesis in Arabidopsis. *Plant J.* **58**, 13-26.
Toller, A., Brownfield, L., Neu, C., Twell, D. and Schulze-Lefert, P. (2008). Dual function of Arabidopsis glucan synthase-like genes *GSL8* and *GSL10* in male gametophyte development and plant growth. *Plant J.* **54**, 911-923.
Torii, K. U. and Clark, S. E. (2000). Receptor-like kinases in plant development. *Adv. Bot. Res. Adv. Plant. Path.* **32**, 226-268.
von Arnim, A. G., Deng, X. W. and Stacey, M. G. (1998). Cloning vectors for the expression of green fluorescent protein fusion proteins in transgenic plants. *Gene* **221**, 35-43.
Wang, H., Ngwenyama, N., Liu, Y., Walker, J. and Zhang, S. (2007). Stomatal development and patterning are regulated by environmentally responsive mitogen-activated protein kinases in Arabidopsis. *Plant Cell* **19**, 63-73.
Willmer, C. M. and Saxton, R. (1979). Stomata and plasmodesmata. *Protoplasma* **100**, 113-124.
Winter, D., Vinegar, B., Nahal, H., Ammar, R., Wilson, G. V. and Provart, N. J. (2007). An "electronic fluorescent pictograph" browser for exploring and analyzing large-scale biological data sets. *PLoS One* **2**, e718.
Yang, T. J., Perry, P. J., Ciani, S., Pandian, S. and Schmidt, W. (2008). Manganese deficiency alters the patterning and development of root hairs in Arabidopsis. *J. Exp. Bot.* **59**, 3453-3464.